GEOSPATIALLY ENABLED AIRBORNE RAPID RESPONSE SYSTEMS: DESIGN, CALIBRATION AND PERFORMANCE ANALYSIS

M. Mostafa[1, *], J. Woolard[2], J. Sellars[2], M. Aslaksen[2], J. Kosofsky[1], and J. Hutton[1]

[1]Applanix Corporation, 85 Leek Cr., Richmond Hill, Ontario, Canada L4B 3B3 – mmostafa, jkosofsky, and JHutton@applanix.com
[2]National Oceanic and Atmospheric Administration, 1315 East West Hwy, Silver Spring, MD 20910 – jason.woolard, jon.sellars, and mike.aslaksen@noaa.gov

Commission I, WG I/9

KEY WORDS: rapid response, photogrammetry, inertial, GNSS, calibration, airborne, direct georeferencing, multi-head camera

ABSTRACT:

The National Oceanic and Atmospheric Administration (NOAA) has been responsible for enabling The United States rapid responders during the hurricane season. Over decades of experience in enabling Rapid Response nationwide resulted in NOAA identifying the detailed engineering requirements for designing the next generation geospatially enabled airborne rapid response systems for aerial survey image capture, georeferencing, and high precision mapping. This paper is focused on presenting the state of the art, new trends, and the performance analysis of NOAA's DSS version 6 for Rapid Response which development and testing took place in 2020/2021.

1. INTRODUCTION

For several decades, the National Oceanic and Atmospheric Administration (NOAA) has assisted with recovery efforts following a variety of natural disasters, including earthquakes, tsunamis, and hurricanes. In the early days, NOAA used aerial film cameras to survey areas affected by these events, which meant key information about the extent of damage to structures and the environment would not be known for days. Since then, NOAA has been researching and utilizing emerging technologies to produce geospatially accurate information as quick as possible to better enable rapid repose efforts (c.f., Brennan and Lander, 1991; White and Aslaksen, 2006).

As a result of these efforts, NOAA pioneered the use of fully digital directly georeferenced aerial surveys for Rapid Response (c.f., White and Aslaksen, 2006).

2. NOAA'S RAPID RESPONSE SYSTEM DESCRIPTION

From their years of experience in collecting and providing Rapid Response imagery nationwide and performing aerial surveys of the national shoreline, NOAA identified the detailed engineering requirements for designing the next generation geospatially enabled airborne mapping system that could be used optimally for collecting both rapid response imagery and traditional imagery for shoreline mapping.

The system design, development, and testing took place during 2020 and 2021 which was logistically challenging due to many imposed restrictions caused by the Covid-19 pandemic.

NOAA's DSS V6 system design includes: two PhaseOne RGB 150 Megapixel cameras, two PhaseOne NIR 100 Megapixel cameras, an Applanix POS AV 610 direct georeferencing system, and a flight management system. The system comprises two camera pairs with one RGB and one NIR cameras in each pair.

A unique and novel feature of the system is that each camera pair can be moved by the operator into a nadir or an oblique position during flight. For rapid response missions, both pairs are flown in oblique mode enabling a very large footprint to be collected for efficiency, and with large viewing angle to capture the sides of buildings to better view damage. For traditional shoreline mapping projects, either pair of the cameras is moved to the nadir mode to collect 4 band stereo imagery.

This unique feature of the DSS V6 means a single camera system can be utilized to meet all of NOAA's imagery mandates thus greatly increasing efficiency. Figure 1 shows the system aircraft installation onboard NOAA's King Air Aircraft as well as system operation during airborne surveys.

Figure 1: NOAA's DSS V6 Installed Onboard NOAA's King Air Aircraft (left). Flight Operations Team Managing Airborne Data Acquisition in Real-Time (right)

Figure 2 shows the multi-camera part of NOAA's system installed onboard NOAA's aircraft. Figure 3 shows the cameras during operation. The arrow shown in Figure 3 points in the flight direction. Additionally, Figure 3 shows that the first camera pair in the flight direction (shown on the left-hand side of Figure 3) was adjusted to the nadir position while the second camera pair was adjusted to the oblique position by the operator. Figure 4 shows NOAA's online Rapid Response Portal which is accessible by rapid responders around the entire nation. Figure 4 shows hurricane IDA imagery as an example.

* Corresponding author

Figure 2: NOAA's System Aircraft Installation - The Multi-Camera System Component

The oblique positions for both camera pairs are tilted by 22.5 degrees from the vertical axis. This oblique angle has been one of the parameters that NOAA carefully considered during the system design phase to accommodate the requirements for both Rapid Response and Coastal Zone mapping. Table 1 lists the RGB camera dimensions while Table 2 lists the NIR camera dimensions. Table 3 lists the Trimble Applanix POS AV 610 accuracy specifications.

Please note that the photogrammetric geometry of the RGB camera when coupled with a 60% overlap allows for an excellent Base-To-Height ration suitable for high precision mapping using POS AV 610 in a pure Direct Georeferencing mode.

Table 1: RGB Camera Dimensions

Parameter	*Value*	*Unit*
Image width (across track)	14,204	pixel
Image length (along track)	10,652	pixel
Nominal Focal length	50	mm
Pixel size	3.76	µm

Table 2: NIR Camera Dimensions

Parameter	*Value*	*Unit*
Image width (across track)	11,608	pixel
Image length (along track)	8,708	pixel
Nominal Focal length	50	mm
Pixel size	4.6	µm

Table 3: POS AV 610 Accuracy Specifications

	[1]Post Processed RTX	[2]Post Processed
Position (m)	0.03 H 0.06 V	0.02 H 0.05 V
Roll & Pitch (deg)	0.0025	0.0025
True Heading (deg)	0.005	0.005

[1]Post Processed Trajectory using Trimble PP-RTX global service
[2]Post Processed Trajectory Using a dedicated base station or *SmartBase*^{TM}

Figure 3: NOAA's System Aircraft Installation - The Multi-Camera System Component during Operation

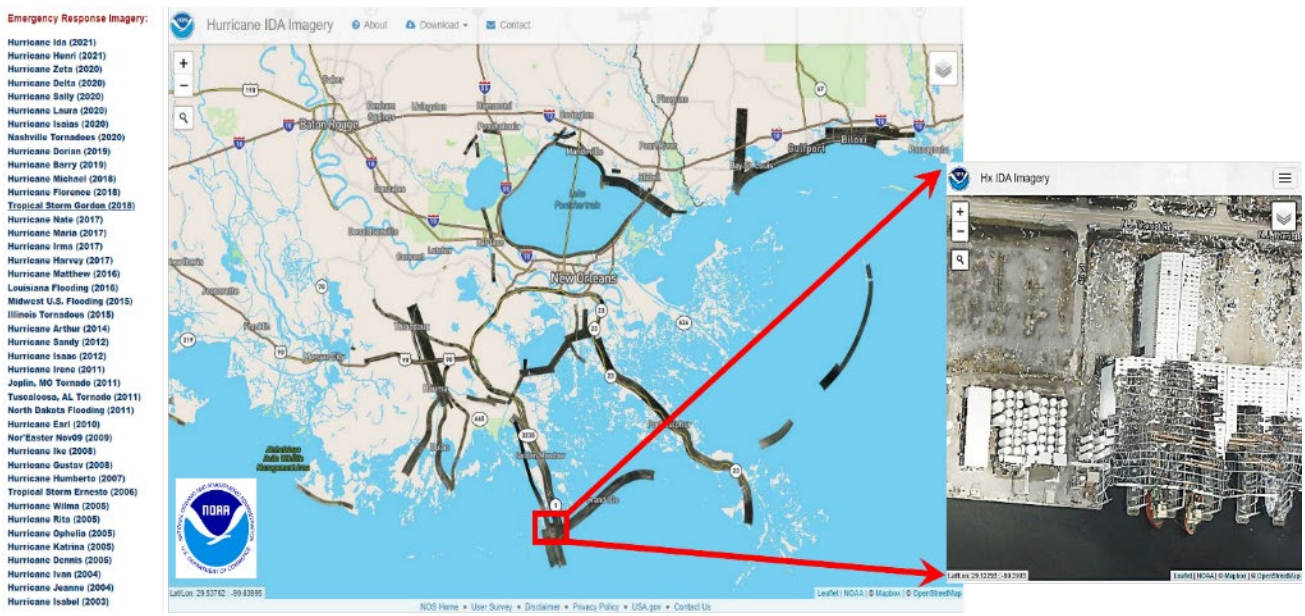

Figure 4: NOAA's Online Portal for Hurricane IDA Imagery - Accessible in Near Real-Time by Rapid Responders (NOAA, 2022: storms.ngs.noaa.gov) – The left panel shows NOAA's List of Emergency Response Imagery since 2003

3. DIRECT GEOREFERENCING

Direct Georeferencing (DG) is the process of computing the ground coordinates for any ground point that appears in an airborne image using inertial/GNSS integrated systems.

DG is a scientific concept that is applicable to any airborne or terrestrial camera once integrated with a GNSS/Inertial system.

Schwarz et al (1993) pioneered DG in the Academia for airborne and terrestrial applications. Successful academic research was published in the 1990s when DG was integrated with many airborne sensors including film cameras (c.f., Škaloud, et al, 1996) or digital cameras (c.f., Mostafa and Schwarz, 2000).

In the commercial environment, Reid, et al (1998) introduced the first professional-grade commercial product to the airborne mapping profession using an IMU-integrated DGPS (c.f., Hutton et al, 1997).

Mostafa (2003) presented the design, development, and performance of the DSS. Mostafa and Hutton (2005) demonstrated the ability of the DSS to operate in a pure DG mode.

Ip and Mostafa (2006) demonstrated that DSS aerial surveys for rapid response operating in a pure DG mode produce near real-time high-quality mapping products, especially when data processing workflows properly addressed the balance between the desired geospatial data resolution, accuracy, and processing time.

NOAA has been using the DSS for Rapid response in a pure Direct Georeferencing mode for over a decade. On the other hand, NOAA's scientists and engineers designed and implemented a seamless and sophisticated data processing workflow that integrates the raw imagery, raw inertial-GNSS data, and the national elevation models to produce high precision orthophotos in near real time without aerial triangulation or ground control.

NOAA's workflow integrates a number of industry standard software packages, open-source software utilities and homemade software tools. The above has been streamlined in order to allow for mass production of high precision maps in near real time. NOAA devised the workflow necessary to do nadir/oblique image integration with inertial-GNSS data while incorporating national elevation models to produce quality orthomosaics without ground control in a pure direct georeferencing environment as shown in Figure 5.

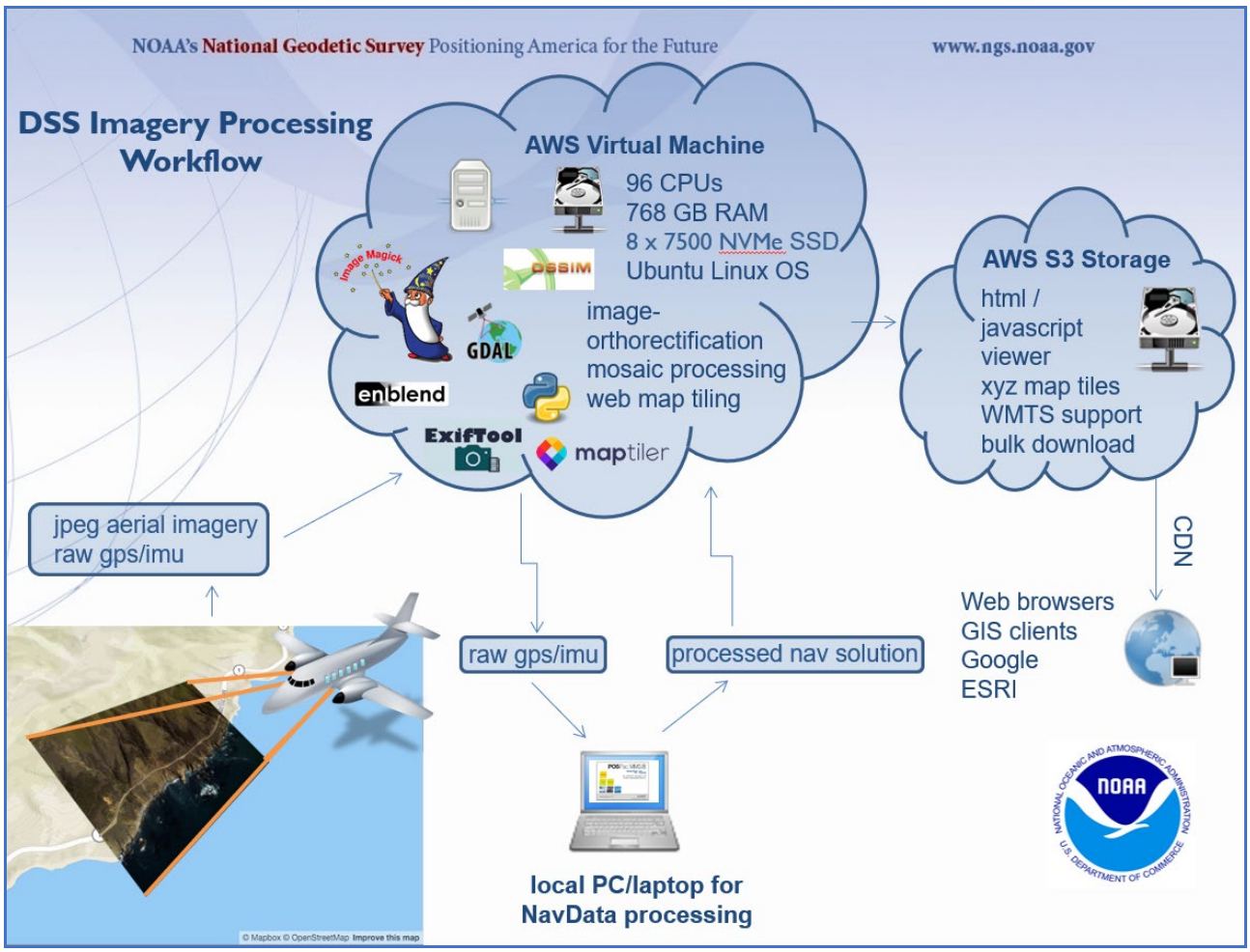

Figure 5: NOAA's Rapid Response Data Acquisition, Processing, and Dissemination Workflow

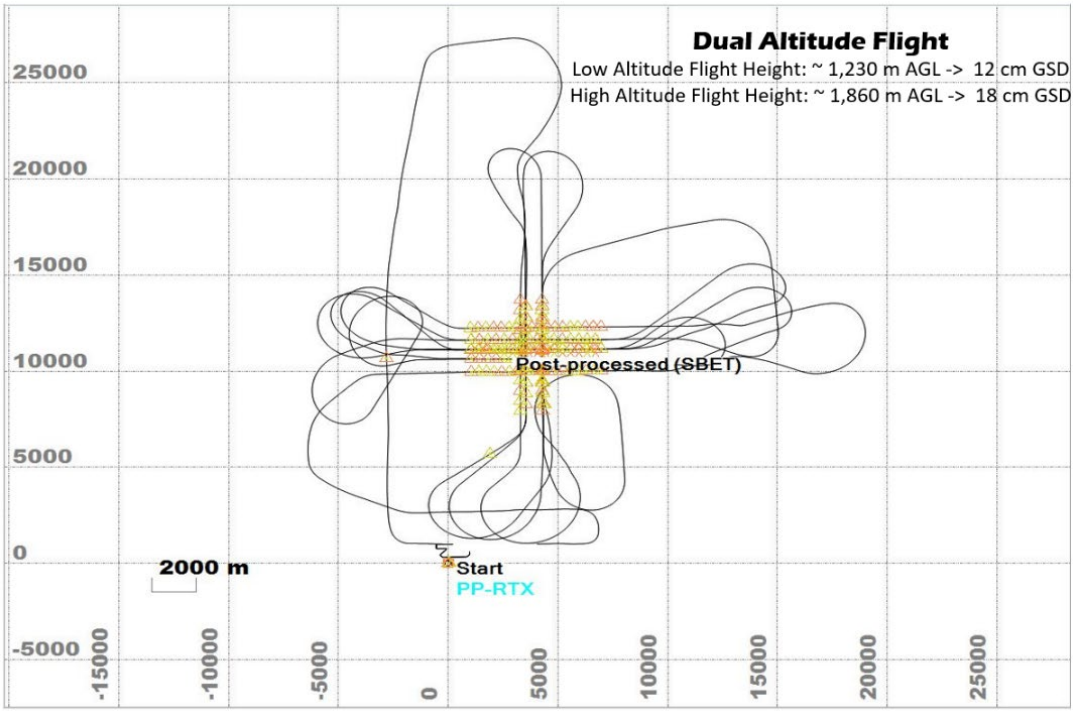

Figure 6: August 5th, 2021 Flight over NOAA's Test Field in Lakeland, Florida

4. CALIBRATION, TESTING, AND ACCURACY ASSESSMENT

During system development, a number of test flights were flown over two of NOAA's test fields in Lakeland, and Gainesville, Florida for system testing, characterisation, validation, performance analysis, and accuracy assessment purposes.

High accuracy ground control was established in NOAA's test fields to be used as check points for independent accuracy checks at different steps of NOAA's processing workflow.

One of the processing workflow aspects is system calibration including boresight, camera, and lever arms. A number of requirements were devised for accurate system calibration during data acquisition and processing including the flight pattern, and the calibration processing mechanism.

Dual-Altitude flights have been proven successful in providing high precision simultaneous camera and boresight calibration (c.f., Mostafa, 2003, Ip et al, 2006 and Casella et al, 2006.) This is due to the fact that a dual-altitude flight containing N-S and E-W flight line establish a strong 3D geometrical network that enables overcoming the mathematical correlation betwee boresight and camera interior orientation.

As a result, a number of dual-altitude flights were flown for system calibration and performance analysis purposes over NOAA's test fields in Lakeland and Gainesville, Florida. One of these flights (flown on August 5th, 2021) is shown in Figure 6.

Five East-West flight lines were flown in the lower altitude and four North-South flight lines were flown in the higher altitude. Each camera imagery together with Applanix POS AV 610 raw data were processed in Applanix POSPac MMS and CalQC softwares.

Instead of using a dedicated GNSS base station to augment the GNSS processing in POSPac to produce cm level accuracy, the POSPac Trimble Centerpoint Post-processed RTX (PP-RTX) service was used. PP-RTX uses corrections derived from a global network of stations operated by Trimble to achieve cm level position accuracy without the need for local base station data.

The corrections are automatically available to POSPac MMS via an internet connection within minutes after the survey. The primary output from POSPac MMS is a Smoothed Best Estimate of Trajectory (SBET) together with the performance metrics which are then used to generate the Exterior Orientation (EO) Parameters for each image at the exact exposure time.

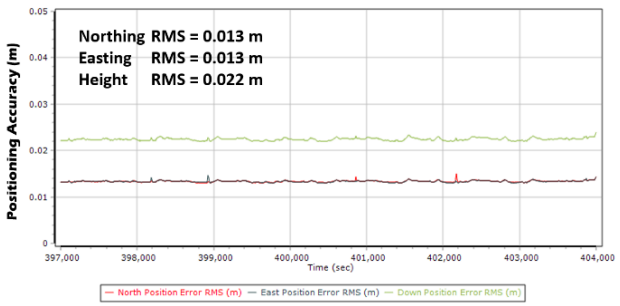

Figure 7: POSPac Results - Positioning Accuracy (m)

Figure 7 shows the positioning accuracy while Figure 8 shows the orientation accuracy. Figure 9 shows the forward/reverse separation which is a recommended QC plot to inspect in POSPac to assess the difference between the trajectory processed forward versus backward in time. The consistency between the forward and reverse solutions indicates that the absolute accuracy of the trajectory is in balance with the RMS of the forward/reverse separation.

In this flight, for example, the forward/reverse separation RMS is about 1 cm for easting and northing and about 2 cm in height, while the *maximum error* occurred at the height component of 5.5 cm as shown in Figure 9, which is within the RMS system specifications listed for in Table 3. These results are typical nowadays with PP-RTX and the Trimble survey grade GNSS systems that include all satellites and frequencies from GPS, GLONASS, BeiDuo, and Galileo satellite positioning and navigation systems.

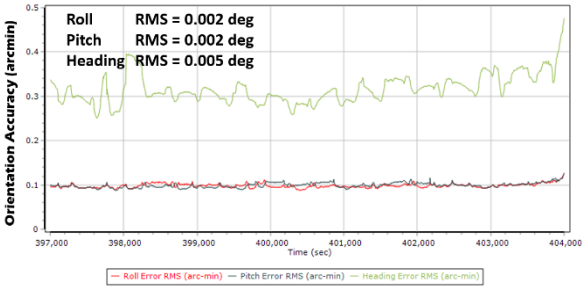

Figure 8: POSPac Results - Orientation Accuracy

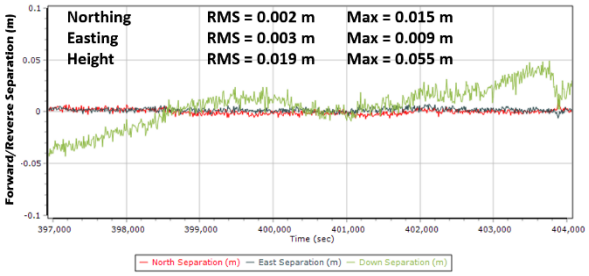

Figure 9: POSPac Results - Forward-Reverse Separation (m)

Figure 10 shows the selected flight lines used to calibrate the system from the Aug 5th, 2021 test flight data.

A total of twenty four check points were established by NOAA in its test field in Lakeland, Florida represented by triangles in Figure 10).

These check points were used to assess the system accuracy during system calibration.

Figure 10: Flight Lines and Check Points (represented by Triangles) for the August 5th NOAA Flight

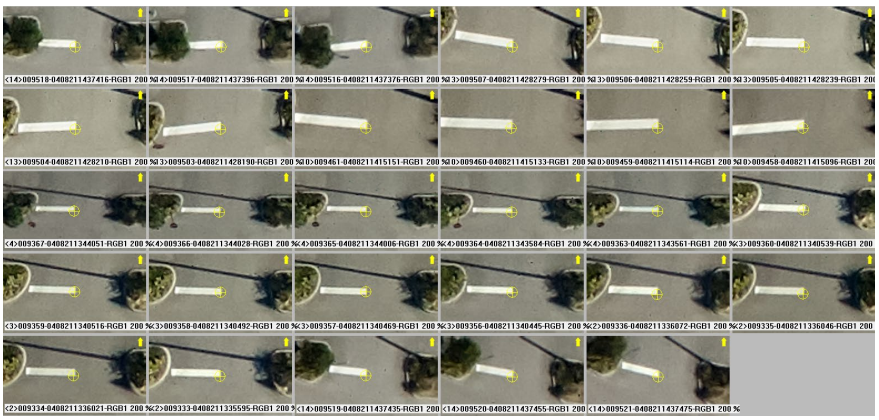

Figure 11: Check Point Automated Measurement in CalQC

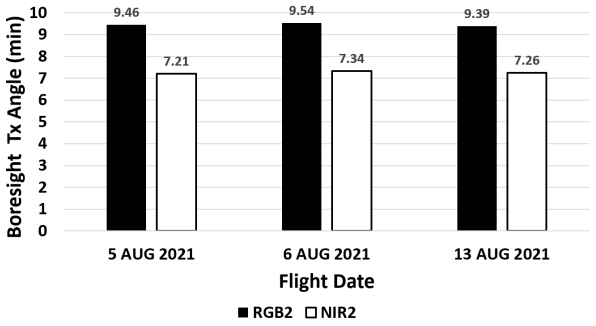

Figure 12: Boresight Calibration for three Flights – Tx

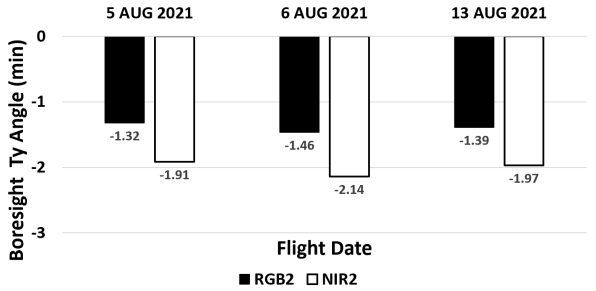

Figure 13: Boresight Calibration for three Flights – Ty

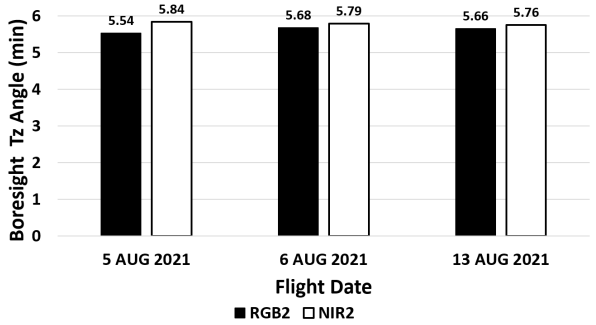

Figure 14: Boresight Calibration for three Flights – Tz

Since the system has four cameras and one IMU, it was necessary to assess the rigidity of mounting the cameras and the IMU.

This is due to the fact that the boresight angles between each camera and the IMU are always assumed constant during data processing. Therefore, making sure that boresight does not change between flights was one of the testing parameters.

In order to assess the boresight calibration stability, and repeatability from different flights, three flights were used. These flights were flown over the same test field in Lakeland, Florida on August 5th, 6th, and 13th, 2021, respectively.

The calibrated values of the three boresight components Tx, Ty, and Tz for the three flights are sown in Figure 12, Figure 13, and Figure 14, respectively for the second camera pair RGB2/NIR2, as an example. The variation of the boresight angles in the three flights has been computed and it is presented in the form of a standard deviation for each boresight component for both RGB2 and NIR2 cameras (of the second camera pair). The computed standard deviations are listed in Table 4.

These results demonstrate that the system boresight calibration computed from three different flights is consistent and repeatable with minimal differences (noise) that is well within the POS AV 610 system specifications.

Table 4: Standard Deviation of the differences between Boresight Angles Computed from Three Flights

Boresight Component	Tx	Ty	Tz
σ_{RGB2} (deg)	0.0012	0.0015	0.0025
σ_{NIR2} (deg)	0.0014	0.0011	0.0026

5. SYSTEM ACCURACY ASSESSMENT

NOAA's DSS V6 is used in two different applications; namely: Coastal Zone Mapping and Rapid Response. The DSS V6 accuracy requirements are higher for coastal zone mapping than Rapid Response since rapid response data typically has the balance of resolution, accuracy, and the required time to generate useful mapping products.

In order to assess the system accuracy, a number of parameters needs to be taken into consideration, including:

- System accuracy for each of the four cameras
- System accuracy for each camera position (nadir versus oblique)
- Accuracy repeatability for different flights
- System absolute versus relative accuracy

Therefore, a number of flights were used to assess the above-mentioned parameters. These flights were planned in such a way, that the system was set to the nadir position. Some other flights were flown while the system was set to the oblique position. Additionally, in some flights, the system operator moved the system from the nadir to the oblique position and then back to the nadir position during flight.

The same 24 check points shown in Figure 10 were used to assess the system accuracy in a number of flights. CalQC was used for this accuracy assessment exercise.

Figure 11 shows the check point automated measurement tool in CalQC. The following flights were used:

- 12 May 2021 flight – Oblique position,
- 14 May 2021 flight – Oblique Position,
- 26 May 2021 flight – first oblique position,
- 26 May 2021 flight – first nadir position,
- 26 May 2021 flight – second oblique position,
- 26 May 2021 flight – second nadir position,
- 9 July 2021 flight – oblique position, and
- 9 July 2021 flight – nadir position.

The check point accuracy is shown in Figure 15 which demonstrates that the X and Y check point RMS for all flights is about one pixel on average, and that the Z check point RMS ranges from 2 to 4 pixels. In each data set, one of the check points was turned into a ground control during processing in order to calibrate a global datum shift and remove it from the data.

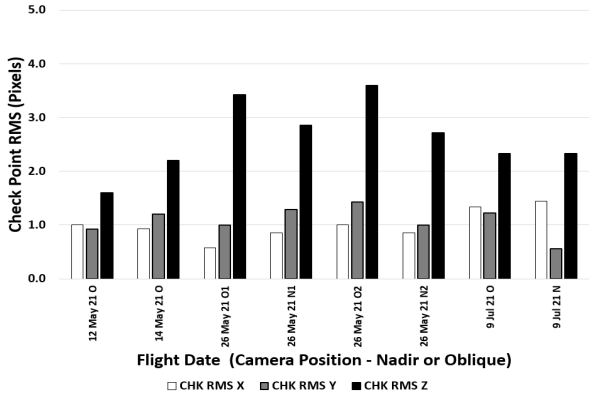

Figure 15: Check Point Accuracy for Various Flights with System Nadir and Oblique Camera Positions

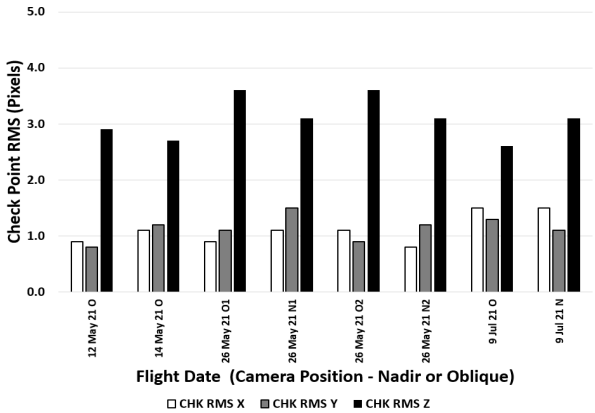

Figure 16: Check Point Accuracy Using One Image Strip for Various Flights with System Nadir and Oblique Camera Positions

NOAA's Rapid Response DSS V6 system is designed to be used to survey disaster areas in any imaging configuration including single or multiple flight lines to cover the desired area. Therefore, the accuracy assessment was done again using only one image strip at a time for each flight.

Figure 16 shows the RMS of check points for all individual single image strips in all of the selected flights in both nadir and oblique camera positions. The results are similar to those when using image blocks to assess accuracy.

NOAA's Rapid Response ortho generation workflow uses pure directly georeferenced imagery together with the national elevation model and camera models as shown in Figure 17.

The workflow starts with importing the POS AV 610 data together with the calibrated boresight angles and the measured lever arms in POSPac MMS. Upon processing the POS AV 610 data, an Exterior Orientation (EO) file is directly generated without the need for a base station which is then directly imported in NOAA's Rapid Response ortho generation workflow along with the camera model and the national elevation data in order to directly produce orthomosaics.

No Aerial Triangulation is done in the process. No ground control is used in the process. This process flow guarantees utmost efficiency and the highest productivity for rapid response. In other words, NOAA's ortho generation workflow uses the latest multi-sensor system technology to generate high quality mapping-grade orthomosaics in near real-time without Aerial Triangulation or ground control.

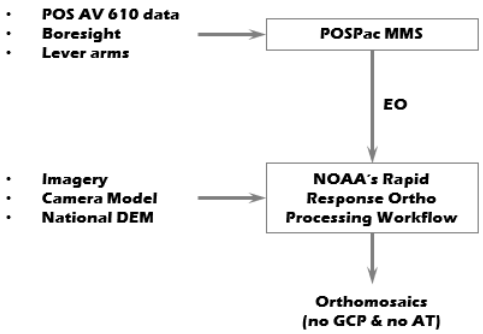

Figure 17: NOAA's Rapid Response Ortho Generation Workflow

Using NOAA's Rapid Response ortho generation workflow shown Figure 17, the orthomosaics were generated for a number of flights. The accuracy of these orthomosaics was assessed against the same 24 check point in Lakeland, Florida shown in Figure 10.

Table 5 lists the orthomosaic check point residuals and their associated statistics for the 5 AUG 2021 flight. The check point RMS for both X and Y is at the level of about 1.5 pixel. This implies that NOAA's orthomosaic generation in near real-time led to deteriorating the check point X & Y RMS from 1 pixel to about 1.5 pixel. This slight deterioration in accuracy due to going from an aerial image domain to a mapping product domain using NOAA's workflow implies that the entire processing workflow is intact and accurate and results in mapping-grade orthomosaics without using Aerial Triangulation or ground control.

In many high precision airborne mapping applications, professional mappers prefer to extract a Digital Surface Model (DSM) using the imagery in order to produce the highest possible accuracy DSM (that typically leverages the existing dense tie points) for ortho generation. However, NOAA's Rapid Response ortho generation software processing workflow uses the national elevation model in order to save the DSM extraction time since time is of an essence in Rapid Response.

6. SUMMARY AND CONCLUSIONS

NOAA's next generation geospatially enabled airborne rapid response system is presented in this paper. NOAA's DSS V6 system design, development, calibration, and testing took place during 2020 and 2021.

The system design includes: two PhaseOne RGB 150 Megapixel cameras, two PhaseOne NIR 100 Megapixel cameras, an Applanix POS AV 610 direct georeferencing system, and a flight management system. The system comprises two camera pairs with one RGB and one NIR cameras in each pair. Each camera pair can be set to either a nadir or an oblique position by the operator at any time during flight.

Several test flights were flown over NOAA's Lakeland and Gainesville, Florida test fields. Both test fields have a well-established network of ground control that were used as check points for accuracy analysis purposes.

Many test flights have been used to calibrate and characterise the system as well as to assess its mapping geometric accuracy. Boresight calibration using the dual-altitude flights including N-S and E-W flight lines was done for multiple flights.

Table 5: Orthomosaic Check Point Residuals (m)

	Check Point ID	dX (m)	dY (m)
Check Points	IMG001	-0.09	0.04
	IMG002	-0.15	-0.04
	IMG006	0.02	-0.01
	IMG007	-0.08	-0.07
	IMG008	-0.13	-0.16
	IMG009	-0.11	-0.08
	IMG010	-0.14	-0.11
	IMG011	-0.11	-0.23
	IMG012	-0.08	-0.16
	IMG013	0.01	-0.02
	IMG014	-0.06	0.04
	IMG015	-0.15	0.11
	IMG016	-0.14	0.03
	IMG017	-0.04	0.06
	IMG018	-0.22	0.01
	IMG023	-0.04	-0.04
	IMG024	-0.10	-0.03
	IMG025	-0.08	0.05
	IMG026	-0.02	0.03
	IMG027	-0.08	0.04
	IMG028	-0.09	0.01
	IMG029	-0.05	0.02
	IMG031	-0.04	0.12
	IMG034	-0.03	0.29
Statistics (m)	**Min**	-0.22	-0.23
	Max	0.02	0.29
	Mean	-0.08	0.00
	σ	0.06	0.11
	RMS	**0.10**	**0.11**
	RMS (pixel)	**1.4**	**1.5**

The results of three of these test flights are presented in this paper. The boresight calibration accuracy proved to be accurate enough for high precision mapping purposes. Comparing the boresight results for the three flights used here showed that their differences are well within the POS AV 610 system accuracy specifications.

Accuracy assessment took place for a number of imaging configurations including image blocks and single strips. The final check point accuracy consistently showed a one-pixel accuracy for X & Y and 2 - 4 pixels for Z in both cases where imagery was used in a block configuration or in a single image strip.

This comparison confirmed that the use of NOAA's DSS V6 for rapid response using any imaging configuration will result in a consistent accuracy when flying one or more image strips to survey a disaster area. NOAA's Rapid Response ortho generation workflow has been used to generate orthomosaics in a pure direct georeferencing environment without Aerial Triangulation or Ground Control to generate an Orthomosaic of the full flight flown on August 5th, 2021.

The ground coordinates of all check points that appeared in the orthomosaic were computed form the airborne data and then compared to the check point land-surveyed coordinates.

The check point RMS was 1.4 and 1.5 pixels, for Easting and Northing, respectively. Therefore, this confirms that NOAA's DSS V6 Rapid Response system produces orthomosaics in near real-time with a mapping-grade accuracy without using Aerial Triangulation or ground control.

REFERENCES

Brennan, A.M., and J.F. Lander, 1991. 2nd UJNR Tsunami Workshop, Honolulu, Hawaii, 5-6 November 1990. Proceedings, https://repository.library.noaa.gov/view/noaa/13447

Casella, V., K. Jacobsen, M.M.R. Mostafa, and M. Franzini, 2006. A European Project on Direct Georeferencing, Proceedings, ASPRS Annual conference, Reno, Nevada, May 1-5, 2006

Fraser, C.S., (1997). Digital Camera Self Calibration, ISPRS Journal of Photogrammetry & Remote Sensing, 52(1997): 149-159.

Hutton, J., Savina, T., and Lithopoulos, L., 1997. Photogrammetric Applications of Applanix's Position and Orientation System (POS). ASPRS/MAPPS Softcopy Conference, Arlington, Virginia, July 27 - 30.

Ip, A.W.L., N. and M.M.R. Mostafa, 2006. A Fully Integrated System for Rapid Response. Proceedings of ISPRS Congress, MAPPS/ASPRS 2006 Fall Conference, San Antonio, Texas, USA, November 6 - 10.

Mostafa, M.M.R., 2007. RapidOrtho™ – A New Tool for Rapid Orthophoto Production for Emergency Response. presented at of the 5th Int. Symp. on Mobile Mapping Technology (MMT2007), Padua, Italy, May 28 - 31, 2007.

Mostafa, M.M.R., and J. Hutton, (2005). A Fully Integrated Solution for Aerial Surveys: Design, Development, and Performance Analysis, PE&RS, 71 (4): 391-399.

Mostafa, M.M.R., 2003. Design and Performance of the DSS. Proceedings, 49th Photogrammetric Week, Stuttgart, Germany, September 1-5, 2003.

Mostafa, M.M.R. and K.P. Schwarz, 2000. A Multi-Sensor System for Airborne Image Capture and Georeferencing. PE&RS, 66 (12): 1417-1424.

NOAA, 2022. NOAA's NGS Emergency Response Imagery Online Portal: https://storms.ngs.noaa.gov

NOAA, 2018. Report to Congress: The National Oceanic and Atmospheric Administration and Department of Homeland Security's Report on National Efforts that Support Rapid Response Following Near-Shore Tsunami Events. https://doi.org/10.25923/q1zh-z042

Reid, D.B., E. Lithopoulos, and J. Hutton, 1998. Position and Orientation System for Direct Georeferencing (POS/DG), Proceedings, Institute of Navigation 54th Annual Meeting, Denver, Colorado, USA, June 1-3, pp. 445-449.

Schwarz, K.P., M.A. Chapman, M.E. Cannon, and P. Gong, 1993. An Integrated INS/GPS Approach to The Georeferencing of Remotely Sensed Data, PE&RS, 59(11): 1167-1674.

Škaloud, J., M. Cramer, and K.P. Schwarz, 1996. Exterior Orientation by Direct Measurement of Position and Attitude, International Archives of Photogrammetry and Remote Sensing, 31 (B3): 125-130.

White, S. and M. Aslaksen, 2006. NOAA's Use of Direct Georeferencing to Support Emergency Response. *Direct Georeferencing Column, PE&RS, Vol. 72 No. 6.*